Original Research

A Four-Channel Electrical Impedance Spectroscopy Module for Cortisol Biosensing in Sweat-Based Wearable Applications

Devangsingh Sankhala[1], Sriram Muthukumar[2], and Shalini Prasad[3] (iD)

Abstract

A four-channel electrochemical impedance spectroscopy (EIS) analyzer module has been demonstrated on flexible chemi-impedance sensors fabricated with gold electrodes for wearable applications. The module can perform time division multiplexed (TDM) impedance measurements on four sensors at 1 kHz. In this work, we characterize the system for the detection of cortisol in an ultralow volume (1–3 µL) of perspired human sweat, sensor performance, and effects during continuous cortisol dosing and with pH and temperature variations expected on the surface of the skin that would be representative of use conditions as seen by a wearable device. Detection of cortisol was shown for concentrations of 1 pg/mL to 200 ng/mL in both synthetic and perspired human sweat, and output response reported as a change in impedance with varying cortisol concentrations. Continuous dose testing was performed to demonstrate the stability of the sensors over prolonged periods of operation for cortisol concentrations within the physiologically relevant range of 10–200 ng/mL reported in human sweat. Temperature and pH effects testing was performed for pH range 4–8 and in a temperature chamber for the clinical range reported on the surface of human skin: 25–40 °C. The cortisol sensor demonstrated stability of operation with 7.58% variability under these conditions.

Keywords

cortisol biosensing, electrochemical impedance spectroscopy, discrete Fourier transform, time division multiplexing, chemi-impedance sensing

Introduction

Wearable healthcare devices are envisioned to be the modern technology that will disrupt methods of diagnosis and significantly enhance human health.[1] These will enable patients to monitor their health themselves, without the need for blood-based diagnostic procedures; take responsibility for their own health; and be better informed about dynamic changes to their health.[2] One important dynamic biomarker expressed in perspired human sweat is cortisol. Adrenal glands produce cortisol, a glucocorticoid, from cholesterol. It is released in response to events and circumstances, such as waking up in the morning, exercising, and acute stress. Cortisol's far-reaching, systemic effects play many roles in the body's effort to carry out its processes and ensure homeostasis. Cortisol secretion of individuals depends on circadian cycle and field environment. Thus, the level of cortisol in the human body is not the same throughout the day. Moreover, cortisol is secreted only in response to physical activity or stressful situations. Laboratory testing techniques would need a daylong study or to take blood/saliva samples several times throughout the day. This

testing method may or may not incorporate response to stressful events. Hence, cortisol detection at point of care is deemed essential to provide personalized healthcare.[3] Efforts are underway to develop wearable detection analytical devices to quantify stress and related abnormalities in environmental condition to gain useful information for appropriate diagnosis and treatment. Studies have linked cortisol levels with human stress, and hence cortisol has recently become a highly relevant biomarker for the detection of physiological stress. As a result, analytical techniques to detect and quantify cortisol levels are of significant

[1]Department of Electrical Engineering, The University of Texas at Dallas, Richardson, TX, USA
[2]EnLiSense LLC, Allen, TX, USA
[3]Department of Bioengineering, The University of Texas at Dallas, Richardson, TX, USA

Corresponding Author:
Shalini Prasad, Department of Bioengineering, University of Texas, Dallas, 800 W. Campbell Rd., BSB 11, Richardson, TX 75080, USA.
Email: Shalini.prasad@utdallas.edu

value. It is in this space that there are many innovative technologies under development.

Saliva has been identified to be the most promising body fluid enabling dynamic testing of cortisol; blood-based cortisol testing identified one time point in the diurnal cycle for determining physiological outcomes based on cortisol levels.[4] Most recently, sweat has started to become an attractive body fluid for supporting the dynamic testing of cortisol levels. In sweat, cortisol concentrations range from 141.7 ng/mL (daytime) to 8.16 ng/mL (nighttime). A strong correlation between cortisol levels in sweat and hair is hypothesized due to the path that cortisol traverses from serum to hair.[5] Various perspired sweat cortisol patches are under development.[6,7] The major constraints to date have been the requirement of large volumes of sweat (> 20 μL) and the inability to report cortisol levels with varying changes to the sweat microenvironment.

Bioelectronics platforms for detecting biomarkers in portable small-volume formats have typically used current/amperometric-based measurement methods. Most notable among these is the flexible electronics platform used for the detection of electrolytes, lactate, and glucose. The challenge in using an amperometric system is the need for a redox-based probing system, which in turn modulates the target biomarker under study.[8,9] While bioelectronics platforms using amperometric detection are easy to design and implement as portable, low-power DC systems, they lack the selectivity/specificity offered by AC systems.[10,11] In 2015, our research group showed the development of an ultra-low-volume flexible biosensor for sweat cortisol determination using AC-based electrochemical impedance spectroscopy (EIS). We have effectively demonstrated sensitivity, specificity, and ultra-low-volume detection (1–3 μL) with this biosensor.[11] In this work, we show the bioelectronic feasibility of integrating the sweat patch with a low-power reporting platform toward proving the feasibility of developing a wearable bioelectronics device for cortisol testing from perspired human sweat using EIS as the measurement method. EIS-based biosensors take advantage of the intrinsic impedance changes in the system in response to probe–analyte binding and hence can perform label-free detection. Like other electrochemical biosensors, these can be easily integrated into standard electronic integrated circuits (ICs).[10,12] They give a vast amount of information at specific frequency points, making it possible to study the effect of molecular interactions and diffusion mechanisms occurring at various distances from the electrode surface.

EIS is highly sensitive to molecular interactions happening close to the electrode surface. It relies on the inherent properties of molecules, which makes EIS-based sensing suitable for the detection of specific molecules, such as proteins, hormones, nucleic acids, and metabolites. EIS allows for real-time detection using the interface impedance with biomolecular interactions as a function of time. Real-time detection allows us to better understand reaction mechanisms and helps us to better estimate the analyte concentration.[13] The possibility of creating integrated EIS biosensors that use ICs for detection makes EIS an attractive candidate for building portable, cost-effective wearable platforms.[14,15] In this work, a flexible chemi-impedance sensor is proposed for sensing cortisol concentrations in 3 μL of synthetic as well as human sweat samples within the clinical range of 10–200 ng/mL using EIS. Moreover, a four-channel EIS module is proposed for implementing a low-voltage, AC-based impedance measurement system. This work also discusses continuous dosing effects and temperature-dependent characteristics of the wearable biosensor.

Materials and Methods

Chemi-Impedance Sensor Fabrication

Figure 1 shows the cross-sectional view of the chemi-impedance biosensor and the formation of the immunoassay on the functionalized surface. The biosensor substrate is a 100 μm thick, flexible nanoporous polyamide substrate (GE Lifesciences, Piscataway, NJ). Gold electrodes were patterned using a shadow mask and deposited using an e-beam cryo-evaporator.[10]

Materials for Implementing Cortisol Assay

Dithiobis(succinimidyl propionate) (DSP) and its solvent DMSO (Thermo Fisher Scientific Inc., Waltham, MA) were prepared at 10 mM volumetric dilution and the sensor surface was incubated with this cross-linker for a period of 3 h. The monoclonal α-cortisol was ordered from Abcam (Cambridge, MA). Cortisol (hydrocortisone) was obtained from Thermo Fisher Scientific. The antibody was diluted in 1× phosphate-buffered saline (PBS; Thermo Fisher Scientific). The cortisol hormone was diluted using synthetic sweat. Synthetic sweat was prepared as per the recipe stated in Table 2 of M. T. Mathew et al.[16] The pH range was varied by varying the concentration of the components. Human sweat was obtained from Lee BioSolutions Inc. (St. Louis, MO), where it was collected from a single human donor with pH~6. No preservatives were added to this product, and it was stored unfiltered at below −20 °C.

Cortisol Sensor Experimental Protocol

A gold surface was functionalized with 3 μL of 10 mmol DSP linker after incubation for 2 h. The PBS wash was carried out followed by a 15 min incubation of 3 μL of 10 μg/mL α-cortisol antibody. Serial dilutions of cortisol in synthetic sweat were prepared to range from 1 pg/mL to 200 ng/mL, which were dispensed after antibody incubation. Each cortisol concentration was incubated for 15 min on the
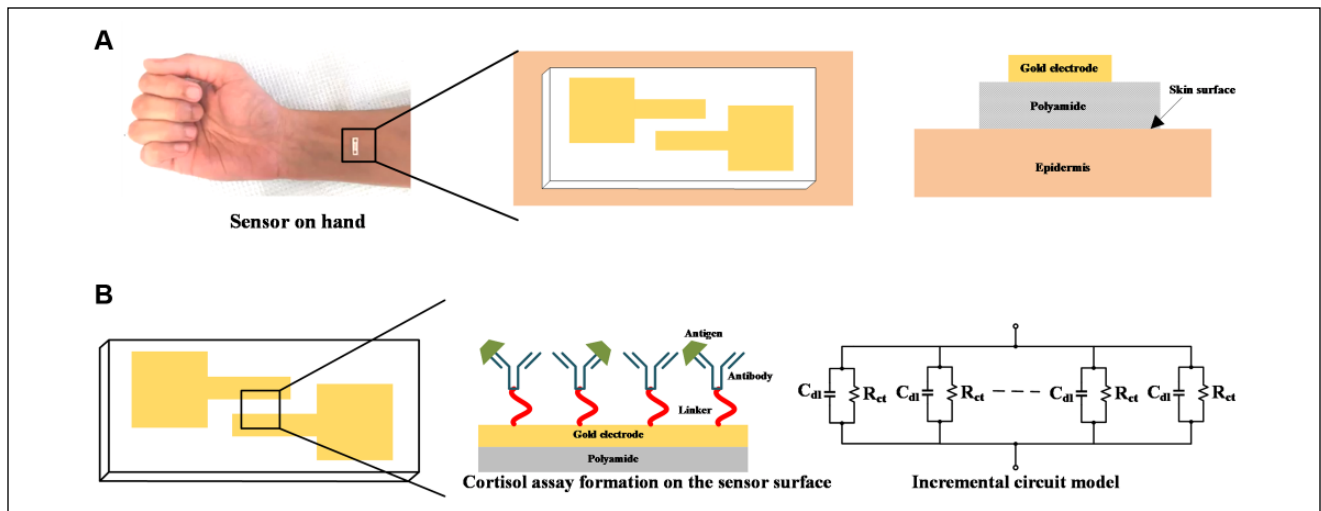
Figure 1. (**A**) Form factor of the proposed chemi-impedance biosensor with a magnified cross-sectional view of the sensor interface. (**B**) Magnified view of the functionalized cortisol assay shown with antigen–antibody binding interaction. Equivalent electrical circuit modeling shown based on double-layer capacitance and charge transfer resistance at single frequency.

sensor surface prior to measurement. The sensor calibration response was obtained in human sweat with increased cortisol concentration doses from 1 pg/mL to 200 ng/mL with $n=4$ replicates of chips. Two test sample chips with 10 and 200 ng/mL cortisol concentration doses on each were also measured. The average readings were then compared with the values obtained from the calibration dose response in human sweat. These EIS measurements were performed by recording the current flow using ADuCM350 after applying 10 mV of AC voltage with a frequency of 1 kHz.

Selection of Measurement Hardware

EIS measurements can be performed using a potentiostat; however, the method of measuring impedance can be based on the Lissajous pattern or discrete Fourier transform (DFT). In the case of the Lissajous pattern, two waveforms are divided, and their phase difference is calculated using *XY* plotting. This is a processor-intensive operation and can take a few seconds to yield results. Moreover, this will only allow one sensor to be connected to the potentiostat unless a multiplexer is used. To show larger throughput and least hardware requirement, a DFT-based time division multiplexed (TDM) sensor module has been used, wherein the measurement time was fixed to 13 ms and impedance measurement was performed on four sensors in quick succession.

Operation of the Sensor Module

The ADuCM350 (Analog Devices Inc., Norwood, MA) system-on-chip (SoC) is at the heart of the measurement setup. The system-level block diagram is shown in **Figure 1**. The SoC consists of a configurable analog front end (AFE), which consists of a wave generator, a switch matrix, and a

2048-point discrete Fourier transform–based impedance analyzer. The amplitude and frequency of the wave generator are fixed using digital words. The AFE is operated using a binary sequence, which controls wave generation, switching sensor channels, and evaluation impedance. The switch matrix enables time division multiplexing of sensors with the instrumentation loop to perform measurement on each sensor. The process of TDM frequency measurement is as follows. The sequence of the instructions is sent to the AFE first-in-first-out (FIFO) buffer using a direct memory access. This helps in achieving low power consumption, as the core processor is not turned on. The wave generator amplitude and frequency are set using respective binary words. Now, the switch matrix connects to a calibration resistor channel to measure the resistance of a precision resistor and uses it as a reference for subsequent measurements. The impedance analyzer block is formed by an I-V converter, analog-to-digital converter (ADC), and DFT engine. The current sensed is converted to a proportional voltage and a 2048-point DFT is performed on it. The real and imaginary parts of the data are converted to magnitude and phase. Two analog pins are selected, from which one acts as a generator and the other as a sink. These pins are in turn connected to one of the sensors due to the switching action of the switch matrix. After a 13 ms DFT cycle on one sensor, the AFE switches to the next sensor channel. Thus, impedance measurement is performed on all four sensors in a combinatorial sequence.

Experimental Setup for Characterizing the Sensor Module

Figure 2B shows the sensor module connected to four biosensors, and the inset shows the flexible biosensor. Twisted-pair wires are used to connect the biosensors to prevent any
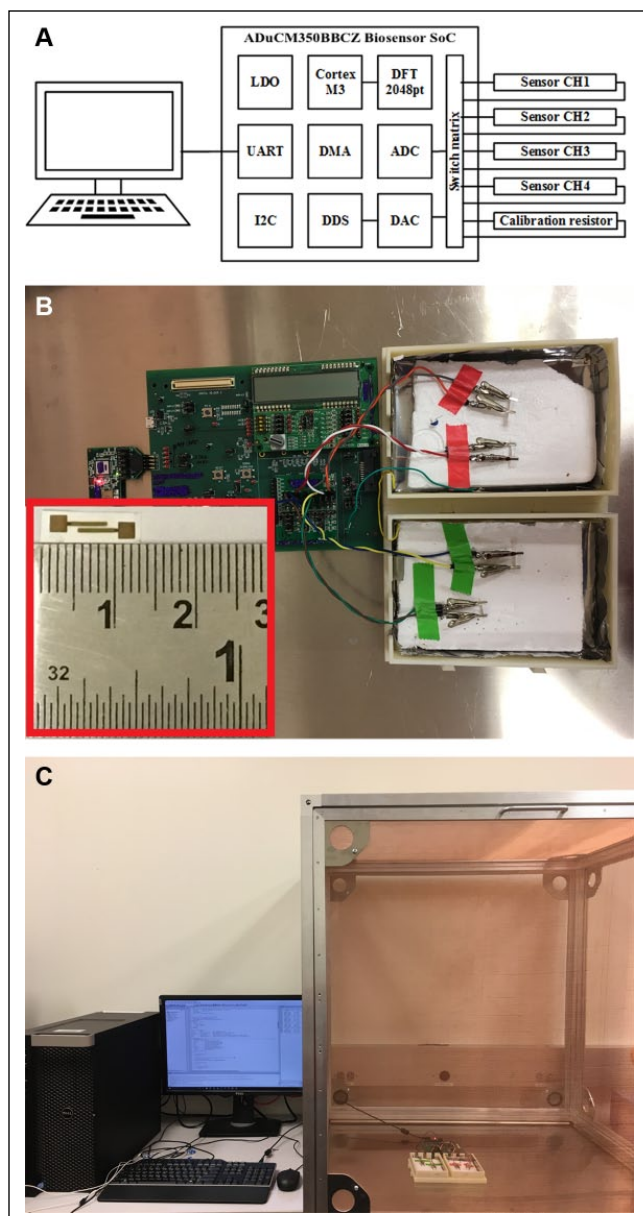
Figure 2. (**A**) Block diagram of the proposed sensor module. (**B**) Sensor module connected to four sensors, one on each channel for multiplexed EIS measurement using the TDM scheme. The acquired measurements were averaged and presented in this work. An enlarged view of the sensor is shown in the inset. (**C**) The sensor module was kept in a Faraday enclosure for low-frequency noise reduction and connected to a PC for data acquisition.

effects of low noise during the measurement process. Additionally, the sensor module is placed in a Faraday cage (Thorlabs Inc., Newton, NJ) for further noise isolation. All measurements are obtained using a serial connection to the PC, as shown in **Figure 2C**. The sample rate for this arrangement is one sample per minute, and all four sensors

are measured for impedance magnitude and phase in rapid succession.

Experimental Setup for Temperature Stability

To demonstrate the stability of sensor impedance over varying temperatures, a temperature chamber (TestEquity LLC, Moorpark, CA) was used to emulate a temperature profile from 25 to 40 °C. **Figure 9A** shows the experimental arrangement for temperature testing, where both the sensor module and the sensors were placed on an insulated surface. A temperature profile ranging from 25 to 40 °C and back to 25 °C was applied twice to the sensor as well as the sensor module. Concurrently, at an interval of 5 min, dose concentrations starting from 10 to 200 ng/mL were dispensed in increments of 10 ng/mL.

Results and Discussion

Calibration of Sensor Module Using Lumped Elements

The sensing module was tested for individual channel offset on the calibration channel of a universal dummy cell (Gamry Instruments, Warminster, PA). Since ADuCM350 is an integrated measurement solution, the channel offset seen is minimum due to manufacturing control. Measured data were collected on a PC using a serial port. **Figure 3A–C** shows the impedance magnitude Z_{mod}, real part Z_{real}, and imaginary part Z_{imag}, respectively, for the dummy cell over a period of 15 min for a sampling rate of one sample per minute. The median of measured Z_{mod} from **Figure 3A** for the four channels was ~3008 Ω, with a variation of ~3 Ω among all medians. **Figure 3B,C** was calculated based on the measured impedance magnitude and phase. The medians for Z_{real} and Z_{imag} were approximately 2843 and –987 Ω, respectively, with a variation of ~5 Ω. The spread of points was within ±10 Ω for each of the given plots. This constituted a 0.33% offset in measurement with respect to the Z_{mod} median value; thus, the offset of each channel was considered negligible.

Error Contribution in Measured Impedance

The spread of measurement obtained from **Figure 3A–C** shows the error contribution from the sensor module, which was taken as approximately ±10 Ω over four channels. This proves good precision of the sensor module. Thus, the analyzer module's error contribution can be subtracted from the total error contribution to find the biosensor's error contribution. The dose calibration response is shown in **Figure 4A–C**. This can be expressed as shown in equation 1 and holds true, as the sensor module and sensor can be modeled as uncorrelated noise sources.[17–19] This expression holds for all measurements performed thereafter as well.
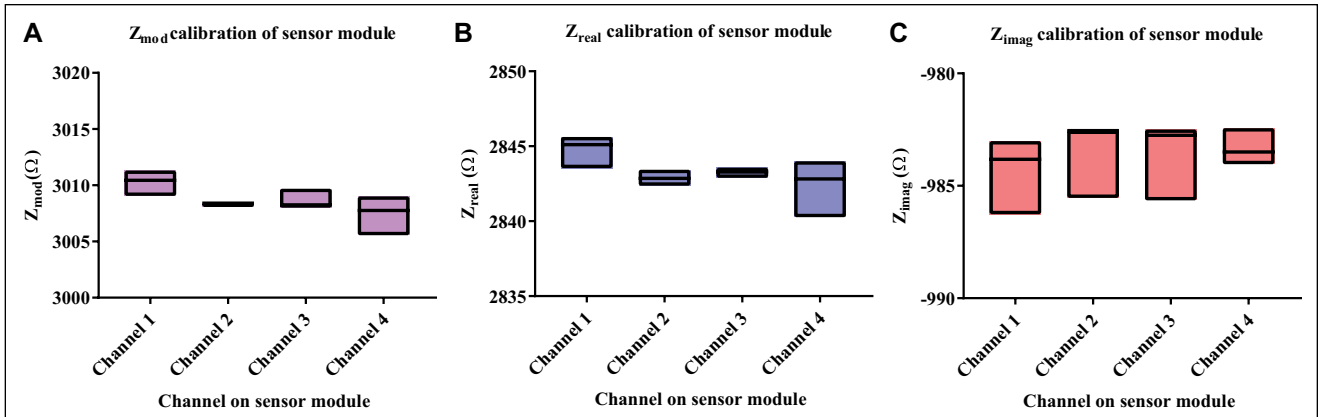
Figure 3. Spread of measured parameters obtained while calibrating individual channels of the sensor module using a dummy cell. (**A**) Z_{mod}. (**B**) Z_{real}. (**C**) Z_{imag}. The measured spread is within $\pm 10\ \Omega$ for each sensing channel.

$$Error_{total} = Error_{sensor\ module} + Error_{sensor} \qquad (1)$$

By using subtractive correction on the dose calibration response, the impact on the accuracy of measured impedance is discussed in all subsequent results sections.

Calibration of Sensor Module Using Synthetic Sweat

Nonfaradaic EIS measurements showed binding between cortisol and its antibody based on the change in the double-layer capacitance. For calibration of the sensor module, cortisol concentrations from 1 pg/mL to 200 ng/mL in synthetic sweat buffer for pH 4 and 8 corresponding to the low and high pH values typical of human sweat (**Table 1**). All experiments were performed in the dark at room temperature. The hardware setup was programmed to measure impedance from four sensors using a 10 mV RMS sine wave at a frequency of 1 kHz. Allowing for greater than 10 times the Nyquist sampling rate for good accuracy of the AFE output, and correlated with previous work from our lab using an ultrasensitive benchtop potentiostat system (Gamry Reference 600, Gamry Instruments), we have established that 1 kHz is an optimal frequency for detecting cortisol using the EIS system.[10] **Figure 4A–C** depicts measured Z_{mod}, Z_{real}, and Z_{imag}, respectively, for cortisol concentrations, averaged over four replicates, each connected to one channel of the sensor module. Polynomial quadratic fit was performed for average Z_{mod} and Z_{imag} for concentrations from 10 ng/mL to 200 ng/mL, as shown in **Table 2**. The function of Z_{mod} ranging from 1 pg/mL to 1 ng/mL showed measured impedance ranging from 2500 to 1300 Ω. For Z_{imag} measurements in synthetic sweat buffer of pH 8, the concentrations in 1 pg/mL to 1 ng/mL showed a quadratic function from 1450 to 1050 Ω. The function is linear for 10 to 200 ng/mL, showing impedance from 800 to 750 Ω.

Since Z_{mod} is a function of Z_{real} and Z_{imag}, and the percentage change of impedance is similar to Z_{mod} and Z_{imag}, it can be proved that cortisol concentration modulates Z_{imag}. Here, a linear correlation was shown from 10 to 200 ng/mL for measured Z_{imag}, thus establishing a linear dynamic range of response for the physiological range of cortisol.

Calibration of Sensor Module Using Human Sweat

EIS measurements were performed for cortisol concentrations from 1 pg/mL to 200 ng/mL in human sweat. **Figure 5A,B** shows measured Z_{mod} and Z_{imag} averaged over four replicates. Polynomial quadratic fit was performed for average Z_{mod} and Z_{imag} for concentrations from 10 to 200 ng/mL, as shown in **Table 2**. For concentrations ranging from 1 pg/mL to 1 ng/mL, Z_{imag} varies from approximately -1800 to $-1050\ \Omega$. For 10 to 200 ng/mL, the variation of Z_{imag} is approximately -1050 to $-1030\ \Omega$. The clinically established cortisol concentration in human sweat has been reported to be in the range of 8–140 ng/mL.[3] Thus, sensitivity to variation in cortisol concentration is established for the biosensor using the EIS analyzer module. Comparing **Figures 4C** and **5C**, the slope is less prominent in human sweat due to the presence of a multitude of ions and other metabolites.[20]

Continuous Dose Testing for Chemi-Impedance Sensor

The robustness of the sensor module to function as a sweat patch for continuous measurements was studied by continuous dosing of the sensor over a period of 60 min using the EIS analyzer module. EIS measurements were taken at the rate of one measurement per minute. This measured impedance of each sensor was normalized over the baseline impedance $Z_{baseline}$, which is defined as the impedance of the functionalized assay at time $t = 0$. The test results were
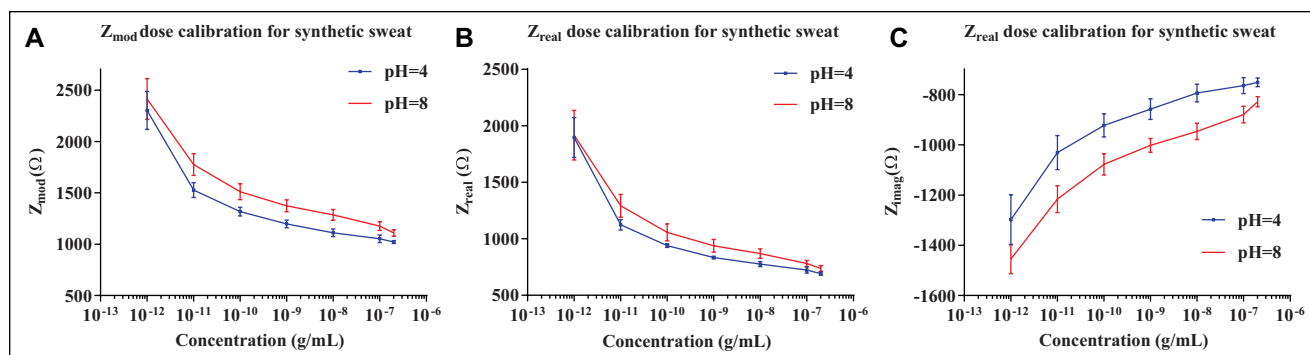
Figure 4. Average of measured impedance for dose calibration of the sensor module for synthetic sweat buffer of pH 4 and 8. (**A**) Z_{mod}. (**B**) Z_{real}. (**C**) Z_{imag}. Dose calibration response shows differentiation from buffer pH and cortisol dose concentrations.

Table 1. Conductivity of the Buffers Used for Dose Calibration.

Buffer	Conductivity, mS/cm
Synthetic sweat, pH = 4	11.4
Synthetic sweat, pH = 8	11.7

averaged over four sensors, where one sensor was connected to each channel. Thus, the normalized change in impedance was calculated as given in equation 2:

$$fractional\ change\ in\ Z = \frac{Z_{concentration} - Z_{baseline}}{Z_{baseline}} \qquad (2)$$

This expression was used to evaluate average changes in Z_{mod} and Z_{imag}. **Figure 6A,B** shows the fractional change in Z_{mod} and Z_{imag}, respectively, for four dose concentrations in synthetic sweat buffer at pH 4, while **Figure 6C,D** shows the fractional change for pH 8 over a period of 60 min. For each dose concentration shown, the dose was introduced at intervals $t = 0$, 15, 30, and 45 min, respectively. Since the antigen–antibody binding interaction produces a smaller change to the electrical double layer for lower concentrations,

the conductivity of the assay decreased. At zero continuous dosing, due to no desirable interaction, the drying of the chip shows a large decrease in fractional change of Z_{mod} and Z_{imag}. The measured fractional Z_{imag} change of the biosensor for a 10 ng/mL cortisol concentration at pH 4 is ~35%. With higher concentrations of 100 and 200 ng/mL, due to more binding interaction, the capacitive behavior of the biosensor becomes less prominent; thus, a fractional change of 25% and 23% was observed.

The measured impedance for pH 4 translated to an equivalent RC circuit combination and is depicted in **Figure 7A,B**, which shows that the change in Z_{imag} is more prominent for the proposed biosensor due to changes in double-layer capacitance. The spread of the measured impedance values is shown in **Figure 8A,B** for pH 4 and **Figure 8C,D** for pH 8. The interquartile regions depict impedance over a period of 60 min and show that the sensor module can differentiate different dose concentrations. It can be seen that for 10 ng/mL, the spread of the measured Z_{imag} is 150 Ω due to lower binding interaction. With a higher binding interaction at 100 and 200 ng/mL, the spread reduces to 50 and 100 Ω. Thus, the spread of measured points depicts the ability of the sensor module to differentiate between the presence and absence of cortisol.

Table 2. Summary of Polynomial Fit Performed on Z_{mod} and Z_{imag} for Synthetic Sweat Buffer for pH 4 and 8 at Room and Elevated Temperatures and Human Sweat at Room Temperature.

	Synthetic Sweat pH 4 25 °C		Synthetic Sweat pH 8 25 °C		Human Sweat pH ~6 25 °C		Synthetic Sweat pH 4 >25 °C		Synthetic Sweat pH 8 >25 °C	
	R^2	CV%	R^2	CV%	R^2	CV%	R^2	CV%	R^2	CV%
Z_{mod}	0.9845	6.35	0.9953	0.47	0.9162	8.38	0.7016	29.84	0.608	39.2
Z_{imag}	0.994	2.34	0.9994	0.6	0.9914	0.86	0.9288	7.12	0.9242	7.58

R^2 values and variability are given using a second-order polynomial fit for the physiological range of sweat cortisol concentration.
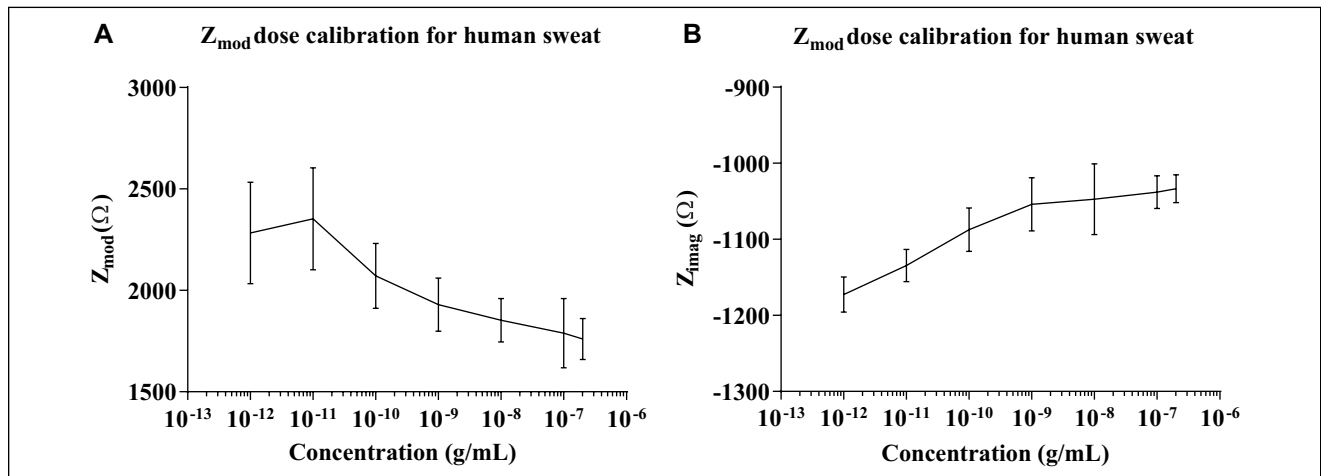
Figure 5. Average of measured impedance for dose calibration of the sensor module for human sweat buffer at pH 6. (**A**) Z_{mod}. (**B**) Z_{imag}.
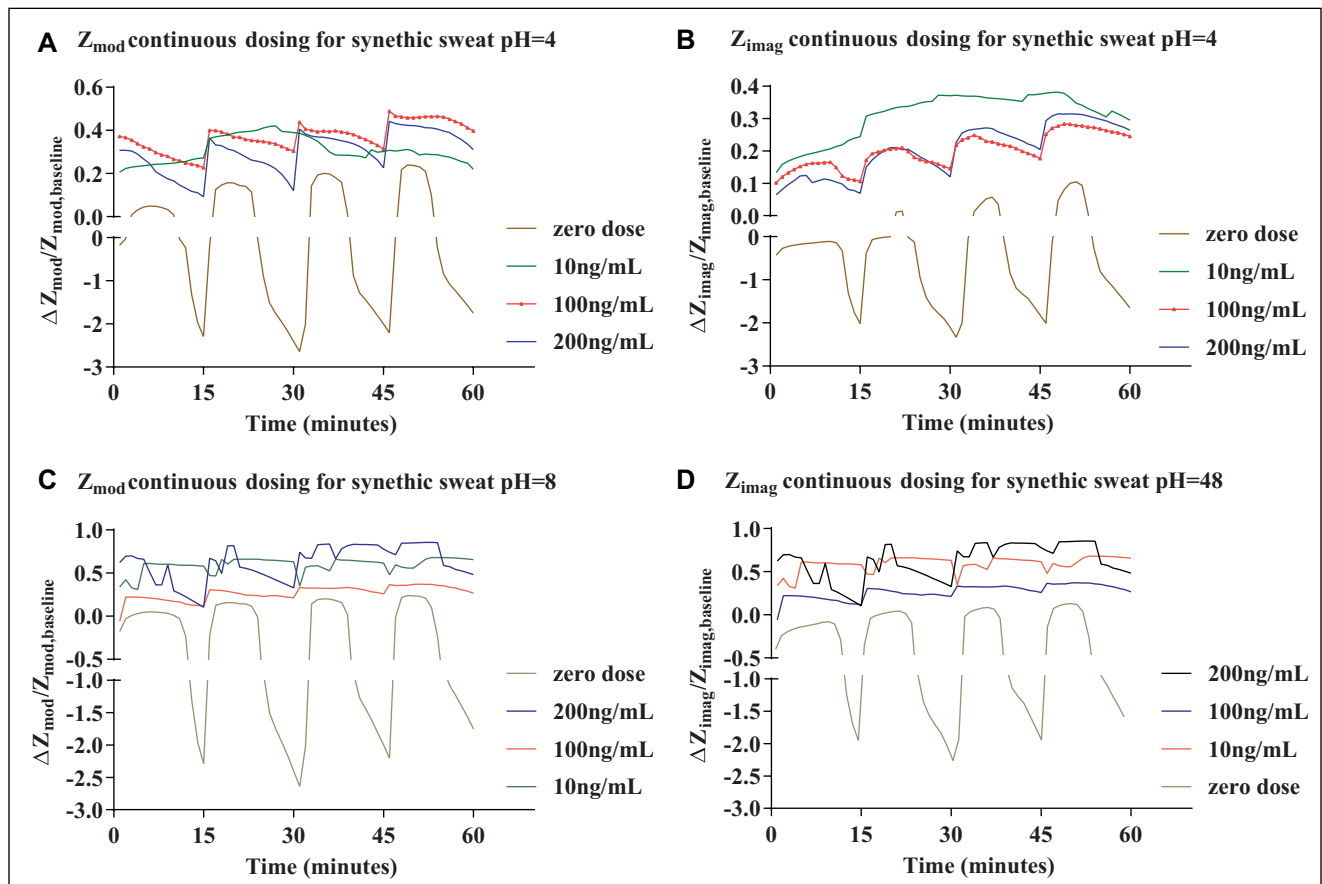

Figure 6. Fractional change in average measured impedance for continuous dose testing in synthetic sweat buffer. The dose was dispensed at an interval of 15 min for the sensors under test. Fractional change of Z_{mod} (**A**) and Z_{imag} (**B**) for pH 4. Fractional change of Z_{mod} (**C**) and Z_{imag} (**D**) for pH 8.
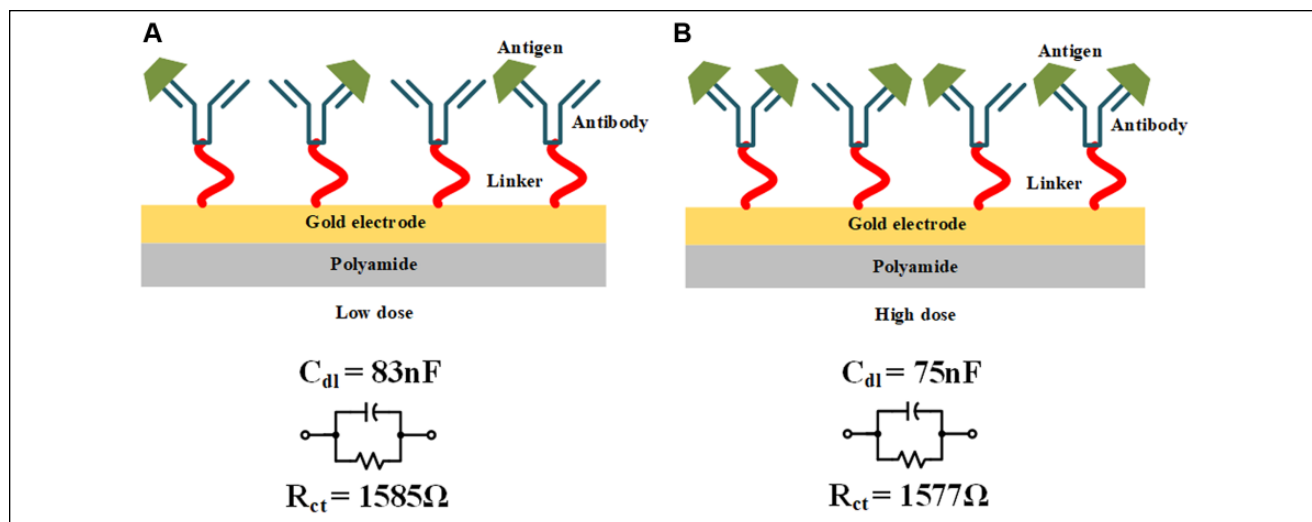
Figure 7. Visual representation of antigen–antibody binding at the sensor interface during low-dose and high-dose concentrations. Averaged PSPICE model for the biosensor under continuous dose testing for synthetic sweat buffer at pH 4 for (**A**) low dose and (**B**) high dose. The PSPICE model shows change in capacitance.
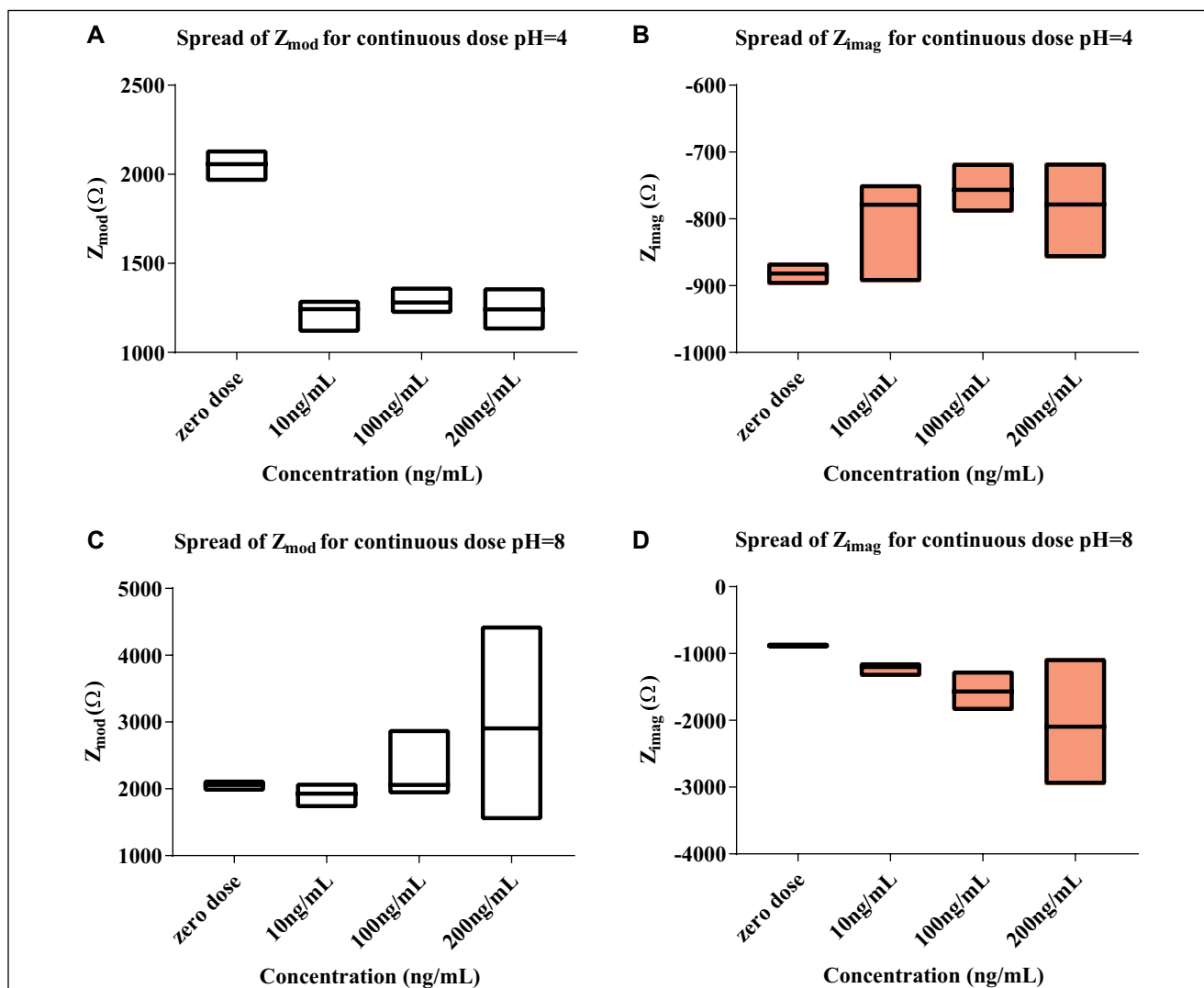

Figure 8. Spread of measured parameters for continuous dose testing. (**A**) Change of Z_{mod}. (**B**) Change of Z_{real}. (**C**) Change of Z_{imag}. The spread shows distinguishable interquartile regions for 0, 10, and 100 ng/mL cortisol dose concentrations for a simulated dynamic monitoring scenario.
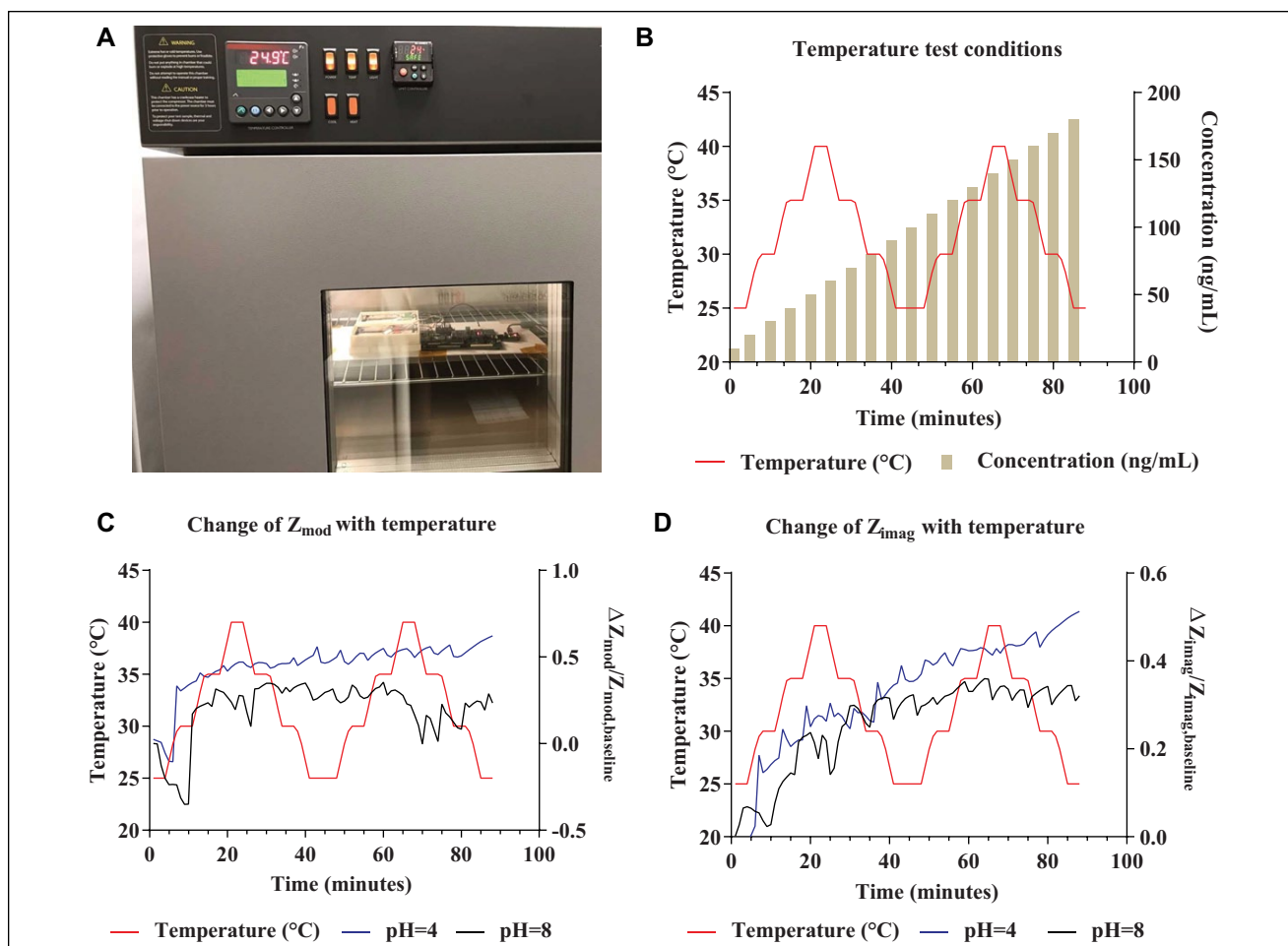
Figure 9. (**A**) The sensor module was connected to four biosensors and placed in the temperature chamber for temperature testing. The change of measured impedance parameters was recorded, along with instantaneous temperature. Cortisol doses made in synthetic sweat buffer of pH 4 and 8 were used for this experiment. (**B**) The test conditions for temperature study include an increase of dose concentration every 5 min and change of temperature as per a profile. (**C**) Fractional change of Z_{mod}. (**D**) Fractional change of Z_{imag}. The change in Z_{imag} is a quadratic function corresponding to an increase in cortisol dose concentration irrespective of change in temperature.

Temperature Stability of Chemi-Impedance Sensor

The goal of the sensor is to function as a wearable device; hence, assessing its performance over a wide range of temperatures from room temperature to elevated body temperature is important. **Figure 9B** shows the test conditions set for the temperature study, in which a temperature profile ranging from 25 to 40 °C and back to 25 °C was applied twice to the sensor as well as the sensor module. Concurrently, at an interval of 5 min, dose concentrations starting from 10 to 200 ng/mL were dispensed in increments of 10 ng/mL. **Figure 9C,D** shows measured fractional change in Z_{mod} and Z_{imag} for synthetic sweat buffer for pH 4 and 8. The measured change of Z_{imag} was fit to a second-order polynomial with R^2 of ~0.92. **Table 2** shows the R^2 and the variability of the fractional change

function of Z_{imag} measured over a period of 90 min. Based on this R^2 value, a variability of ~7.6% from the ideal second-order polynomial fit was shown for a temperature range of 25–40 °C for repetitive temperature cycles.

Conclusions

Wearable lancet-free and label-free biosensors based on human sweat are novel devices that can detect various disorders in the human body; one such important biomarker is cortisol. Various amperometry techniques, such as chronoamperometry and cyclic voltammetry, employ a large potential difference to measure the change in impedance corresponding to the biomarker of interest with a high signal-to-noise ratio. Due to a transient in voltage, the measurement device will experience a large transient, causing

Table 3. Electrical Design Comparison of This Work with Previous Publications.

	Kim et al.[22]	Gao et al.[23]	Umasankar et al.[24]	This Work
Technique	Chronoamperometry	Chronoamperometry	Chronoamperometry	EIS
Analyte	Alcohol	Glucose, lactate, electrolytes	Alcohol	Cortisol
Primary amplifier	LMP9100	LT1462	LMP91000	ADuCM350
Number of ICs in sensing loop	3	18	5	1
Number of channels	2	6	1	4
Measurement time	60 s	60 s	500 s	13 ms

instability and errors in measurement. Moreover, due to the larger settling time of the current, density gradients cause undesirable convective disruption of the diffusion layer.[21] This in turn disrupts the diffusion layer, leading to a larger drawing of current as per Cottrell's equation. However, to develop a bioelectronics interface that captures the dynamic changes to cortisol in human sweat, there is a need to develop a method of measuring impedance changes from arrays of sensors enabling larger throughput. EIS enables measurement of the nonfaradaic impedance modulations occurring at the electrode–electrolyte interface in a dynamic manner without disruption of the affinity capture probes, hence offering a robust sensor platform suitable for continuous monitoring of dynamic changes to cortisol levels.

The four-channel EIS sensor analyzer module that has been presented in this work is capable of sensing cortisol concentrations in both synthetic and human sweat using gold-based flexible, wearable biosensors. **Table 3** shows an electrical comparison of this design with preview publications. It is evident that the proposed sensor platform design is more efficient in terms of implemented active silicon and is capable of being further miniaturized. Moreover, a 13 ms measurement time per channel makes it the fastest measurement device reported to date. We believe that this is the first multiplexed EIS platform capable of translation to a wearable device reported in the literature. The accuracy of the biosensor module was established using dose calibration response in synthetic sweat for pH 4 and 8, as well as for human sweat at pH ~6. Moreover, correction of measured impedance from the sensor module was proposed using the inherent error contribution of the sensor module. Furthermore, sensing of the presence or absence of cortisol for continuous dosing of the biosensor was confirmed using synthetic sweat for pH 4 and 8. In addition, temperature cycle testing was performed to show stability of the sensor for variation of temperature cycles for a range of 25–40 °C with ~7.6% variability on a second-order polynomial fit.

ORCID iD

Shalini Prasad https://orcid.org/0000-0002-2404-3801

References

1. Mukhopadhyay, S. C. Wearable Sensors for Human Activity Monitoring: A Review. *IEEE Sens. J.* **2015**, *15*, 1321–1330.
2. Piwek, L.; Ellis, D. A.; Andrews, S.; et al. The Rise of Consumer Health Wearables: Promises and Barriers. *PLoS Med.* **2016**, *13*, e1001953.
3. Kaushik, A.; Vasudev, A.; Arya, S. K.; et al. Recent Advances in Cortisol Sensing Technologies for Point-of-Care Application. *Biosens. Bioelectron.* **2014**, *53*, 499–512.
4. Singh, A.; Kaushik, A.; Kumar, R.; et al. Electrochemical Sensing of Cortisol: A Recent Update. *Appl. Biochem. Biotechnol.* **2014**, *174*, 1115–1126.
5. Sharpley, C. F.; McFarlane, J. R.; Slominski, A. Stress-Linked Cortisol Concentrations in Hair: What We Know and What We Need to Know. *Rev. Neurosci.* **2011**, *23*, 111–121.
6. Anastasova, S.; Crewther, B.; Bembnowicz, P.; et al. A Wearable Multisensing Patch for Continuous Sweat Monitoring. *Biosens. Bioelectron.* **2017**, *93*, 139–145.
7. Prunty, H.; Andrews, K.; Reddy-Kolanu, G.; et al. Sweat Patch Cortisol—A New Screen for Cushing's Syndrome. *Endocrine Abstracts* **2004**, *7*, 202.
8. Jia, W.; Bandodkar, A. J.; Valdés-Ramírez, G.; et al. Electrochemical Tattoo Biosensors for Real-Time Noninvasive Lactate Monitoring in Human Perspiration. *Anal. Chem.* **2013**, *85*, 6553–6560.

9. Nyein, H. Y. Y.; Gao, W.; Shahpar, Z.; et al. A Wearable Electrochemical Platform for Noninvasive Simultaneous Monitoring of Ca2+ and pH. *ACS Nano* **2016**, *10*, 7216–7224.

10. Munje, R. D.; Muthukumar, S.; Selvam, A. P.; et al. Flexible Nanoporous Tunable Electrical Double Layer Biosensors for Sweat Diagnostics. *Sci. Rep.* **2015**, *5*, 11.

11. Russell, E.; Koren, G.; Rieder, M.; et al. The Detection of Cortisol in Human Sweat: Implications for Measurement of Cortisol in Hair. *Ther. Drug Monit.* **2014**, *36*, 30–34.

12. Wang, Y.; Ye, Z.; Ying, Y. New Trends in Impedimetric Biosensors for the Detection of Foodborne Pathogenic Bacteria. *Sensors* **2012**, *12*, 3449.

13. Vattipalli, K.; Feikert, P.; Brandigampala, S.; et al. Study of Nanoporous Membranes with Applications in the Enhanced Detection of Cadiovascular Biomarker Proteins. *Nano LIFE* **2010**, *01*, 175–183.

14. Manickam, A.; Singh, R.; Ayazian, S.; et al. Front-End Integrated Circuits for High-Performance Biological and Chemical Sensing. In *2011 IEEE 54th International Midwest Symposium on Circuits and Systems (MWSCAS)*, Seoul, Korea, August 7–10, 2011; pp 1–4.

15. Arya, S. K.; Chornokur, G.; Venugopal, M.; et al. Antibody Functionalized Interdigitated μ-Electrode Based Impedimetric Cortisol Biosensor. *Analyst* **2010**, *135*, 1941–1946.

16. Mathew, M. T.; Ariza, E.; Rocha, L. A.; et al. Tribo-Corrosion Behaviour of TiCxOy Thin Films in Bio Fluids. *Electrochim. Acta* **2010**, *56*, 929–937.

17. Hooge, F. N. 1/f Noise Sources. *IEEE Trans. Electron Devices* **1994**, *41*, 1926–1935.

18. Razavi, B. *Design of Analog CMOS Integrated Circuits*. McGraw-Hill: New York, 2001; p 704.

19. Hassibi, A.; Navid, R.; Dutton, R. W.; et al. Comprehensive Study of Noise Processes in Electrode Electrolyte Interfaces. *J. Appl. Phys.* **2004**, *96*, 1074–1082.

20. Munje, R. D.; Muthukumar, S.; Prasad, S. Interfacial Tuning for Detection of Cortisol in Sweat using ZnO Thin Films for Wearable Biosensing. In *2016 IEEE Nanotechnology Materials and Devices Conference*; New York: IEEE, 2016, pp 1–2.

21. Bard, A.; Faulkner, L. *Electrochemical Methods: Fundamentals and Applications*; Hoboken, NJ: John Wiley & Sons, 2001.

22. Kim, J.; Jeerapan, I.; Imani, S.; et al. Noninvasive Alcohol Monitoring Using a Wearable Tattoo-Based Iontophoretic-Biosensing System. *ACS Sensors* **2016**, *1*, 1011–1019.

23. Gao, W.; Emaminejad, S.; Nyein, H. Y. Y.; et al. Fully Integrated Wearable Sensor Arrays for Multiplexed In Situ Perspiration Analysis. *Nature* **2016**, *529*, 509–514.

24. Umasankar, Y.; Jalal, A. H.; Gonzalez, P. J.; et al. Wearable Alcohol Monitoring Device with Auto-Calibration Ability for High Chemical Specificity. In *2016 IEEE 13th International Conference on Wearable and Implantable Body Sensor Networks (BSN)*, San Francisco, CA, June 14–17, 2016; pp 353–358.